

Unification and physical interpretation of the radio spectra variability patterns in Fermi blazars and jet emission from NLSy1s

E. Angelakis, L. Fuhrmann, I. Nestoras, C. M. Fromm, R. Schmidt, J. A. Zensus, N. Marchili, T. P. Krichbaum
Max-Planck-Institut für Radioastronomie, Auf dem Hügel 69, Bonn 53121, Germany

M. Perucho
*Department d'Astronomia i Astrofísica, Universitat de València,
 C/Dr. Moliner 50, 46100 Burjassot, València, Spain*

H. Ungerechts, A. Sievers, D. Riquelme
Instituto de Radio Astronomia Milimétrica, Avenida Divina Pastora 7, Local 20, E 18012, Granada, Spain

L. Foschini
INAF - Osservatorio Astronomico di Brera, Italy

The *F-GAMMA* program is among the most comprehensive programs that aim at understanding the physics in active galactic nuclei through the multi-frequency monitoring of *Fermi* blazars. Here we discuss monthly sampled broad-band radio spectra (2.6 - 142 GHz). Two different studies are presented. (a) We discuss that the variability patterns traced can be classified into two classes: (1) to those showing intense spectral-evolution and (2) those showing a self-similar quasi-achromatic behaviour. We show that a simple two-component model can very well reproduce the observed phenomenologies. (b) We present the cm-to-mm behaviour of three γ -ray bright Narrow Line Seyfert 1 galaxies over time spans varying between ~ 1.5 and 3 years and compare their variability characteristics with typical blazars.

I. BLAZAR VARIABILITY

Among the most prominent characteristics of blazars, is their intense variability at all energy bands from radio to γ -rays and TeV energies. The mechanism producing variability itself depends on the energy band it refers to and has been long debated. The “Shock-in-Jet” model suggested by [1], is broadly accepted to explain the variability in terms of shocks propagating in the jet. The basic assumption is that changes in the particle injection rate, the magnetic field and the bulk Lorentz factor taking place at the jet base, cause the formation of shocks which consequently go through first *Compton*, then *synchrotron* and finally *adiabatic* energy loss phases. An alternative model, the “Internal Shock Model” proposed by [2], suggests that energy is channeled into the jet in an intermittent way. “Plasma shells”, may have different bulk Lorentz factors and masses, so that faster shells can catch up with slower ones, collide with them and create relativistic shocks. The shock accelerates electrons to relativistic energies so that they can emit synchrotron and inverse Compton radiation. Other models explain the variability geometrically. Villata and Raiteri [3] for instance, suggested that orbital motion and jet precession, possibly caused by a binary black hole system, can produce helical jet morphologies which may then cause brightness and spectral variability through changes in the Doppler factor.

Studies of the variability of the *Spectral Energy Distribution* (SED), ideally based on simultaneous datasets, probe the physics driving the energy pro-

duction and dissipation in these systems (e.g. [4, 5]) and can readily reveal some physical parameters such as the brightness temperatures, Doppler factors and the jet viewing angles.

The current report deals with the variability characteristics of AGNs as they are observed in radio bands at cm to mm wavelengths and has a twofold character. First, we present the phenomenological classification of the variability patterns followed by selected *Fermi* blazars and propose a toy-model which can physically explain this classification. Secondly, we present the radio behaviour of three *Narrow Line Seyfert 1* galaxies (hereafter NLSy1) which have been detected in γ -rays by *Fermi*/LAT.

II. THE F-GAMMA PROGRAM

The potential of the LAT, on-board the *Fermi* satellite [6], in the study of AGNs, could be attributed mostly to (a) the covered energy range (from 20 MeV to >300 GeV) and (b) the pace at which the 4π γ -ray sky is being scanned. Given the broadness of the blazar *spectral energy distribution* (SED), the full potential of such densely sampled γ -ray light curves can be explored only when combined with multi-frequency data. Radio monitoring programs are essential in this task since they trace the behaviour of the relativistic jets where both primary and secondary emission processes take place (i.e. synchrotron and inverse Compton processes).

One of the most comprehensive radio monitoring

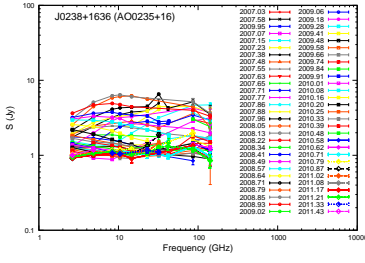


FIG. 1: Prototype source for variability type 1.

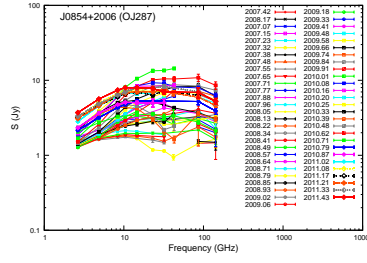


FIG. 2: Prototype source for variability type 1b.

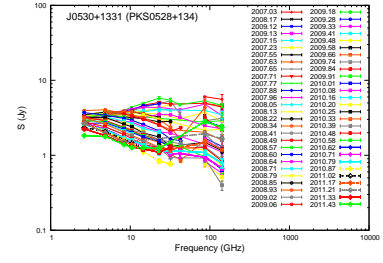


FIG. 3: Prototype source for variability type 2.

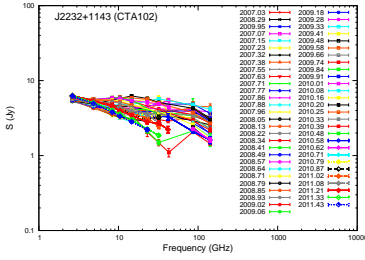


FIG. 4: Prototype source for variability type 3.

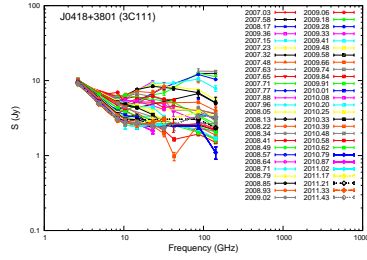


FIG. 5: Prototype source for variability type 3b.

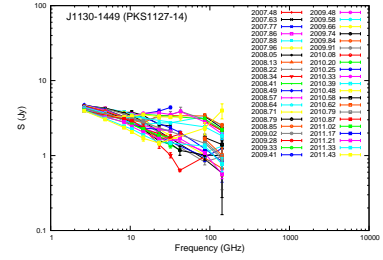


FIG. 6: Prototype source for variability type 4.

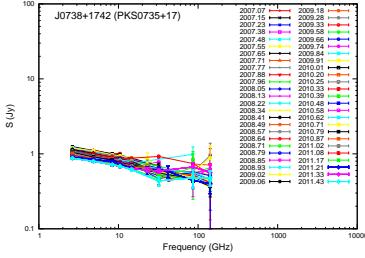


FIG. 7: Prototype source for variability type 4b.

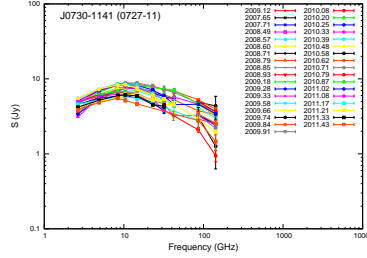


FIG. 8: Prototype source for variability type 5.

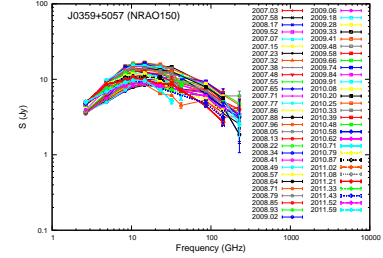


FIG. 9: Prototype source for variability type 5b.

efforts, the *F-GAMMA* program, [7–9] was initiated in 2007 utilising the Effelsberg 100-m, the IRAM 30-m and the APEX 12-m telescopes for the monthly monitoring of ~ 60 *Fermi* blazars at 12 frequencies between 2.6 and 345 GHz. The millimetre observations are closely coordinated with the more general flux monitoring conducted by IRAM at the 30-m telescope. The Effelsberg 100-m telescope is equipped with circularly polarised feeds, while the IRAM 30-m with linearly polarised ones. Details are given elsewhere (Fuhrmann et al. in prep., Angelakis et al. in prep., Nestoras et al. in prep.). Measurements at 4.85 GHz, 10.45 GHz, 32.0 GHz, 86.24 GHz and 142 GHz are done differentially either by using multi-feed systems, or, at IRAM 30-m, by wobbler switching. On average, the time needed for observing an entire spectrum of any given source at Effelsberg alone is of the order of 35 minutes, while at IRAM, roughly 2 minutes. The combined spectra (Effelsberg and IRAM) are observed quasi-simultaneously within

approximately one week. That is, neither the single-facility spectra nor the combined ones are likely to be affected by source variability. In the current study only data collected until June 2011, have been used.

III. BROAD-BAND RADIO SPECTRA VARIABILITY

The data product of the *F-GAMMA* program is monthly sampled broad-band radio spectra covering a frequency range of 2 orders of magnitude. In the following we discuss studies based only on Effelsberg and IRAM data i.e. 2.6 - 142 GHz and present a toy-model for the interpretation of the small number of phenomenological types of variability patterns.

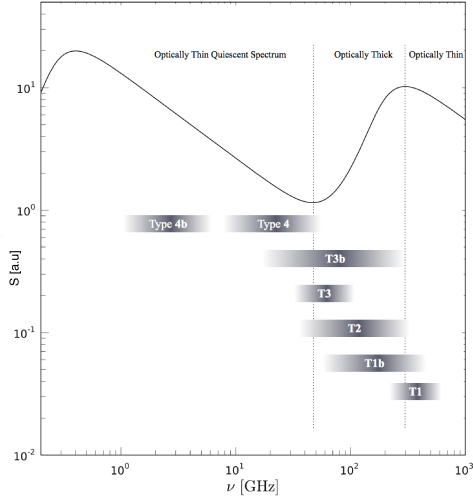


FIG. 10: The assumed two-component system. The different variability types can be reproduced with the appropriate modulation of the relative position and relative broadness of the band-pass denoted by the grey shaded areas.

A. Phenomenological Classification

Angelakis et al. [10, 11] showed that the variability patterns that the source spectra follow as a function of time, fall in a small number of phenomenological classes the prototypes of which are shown in Figures 1 - 9. A detailed description of the characteristics of each type are given in [10, 11]. What is readily obvious in this analysis and can also be seen in Figures 1 - 9, is that the patterns can be basically classified in (a) those characterised by spectral evolution (Figures 1 - 7) and (b) those that show a convex spectrum which varies self-similarly following a close-to-achromatic evolutionary path (Figures 8 and 9).

B. Interpretation of the Observed Phenomenologies

As it is argued in [10], the spectral-evolution dominated types can naturally be explained by a simple two-component system, as it is observed by other programs as well [e.g. 12]. It is shown that a system composed of a steep spectrum component attributed to a large scale jet populated with a varying spectral component, can easily reproduce the observed patterns (Figure 10). The spectral component is assumed to be following the [1] model. Calculations showed that with only a minor coverage of the parameter space that determines the characteristics of those two elements (e.g. intrinsic source luminosity, flare dominance, turnover frequency of quiescent spectrum), is enough to reproduce the observed variability. This discussion refers only to these types that are characterised by spectral

evolution. The “achromatic” behaviour must be attributed to different mechanism as it will be discussed elsewhere.

C. Variability Properties

The different classes discussed earlier have some very fundamental differences. The most obvious one being the increase in the prominence of a quiescent large scale jet as compared to the flaring event with increasing type. That should immediately imprint differences in the distribution of the variability parameters for types that have different quiescent spectrum prominence.

In order to investigate that, we have performed standard variability analysis. For each light curve characteristic variability time scales have been estimated using a structure function analysis described by [13]. These time scales are subsequently used to compute the involved emitting region sizes (assuming the light-travel-time argument) and hence the variability brightness temperatures, as:

$$T_b[\text{K}] = 4.5 \cdot 10^{10} \Delta S \left(\frac{\lambda \cdot D_L}{\Delta \tau \cdot (1+z)^2} \right)^2 \quad (1)$$

where ΔS : the flux density variation in Jy
 λ : the observing wavelength in cm
 D_L : the luminosity distance in Mpc
 $\Delta \tau$: the characteristic time scale in days

Assuming a typical value of $5 \cdot 10^{10}$ K for the upper limit in the brightness temperature on the basis of equipartition arguments [14, 15], we can compute also the variability equipartition Doppler factor, as: $D_{\text{var}} = (1+z) \cdot (T_b/5 \cdot 10^{10} \text{ K})^{\frac{1}{3-\alpha}}$, where α is the spectral index ($S \propto \nu^\alpha$). A typical value of $\alpha = -0.7$ has been used.

In Figure 11 we show the variability brightness temperature (Eq. 1) distribution at three characteristic frequencies, 4.85, 14.6 and 32 GHz, for three groups of sources separately. One group is made of sources of type 3-4 which show the clear presence of a quiescent spectrum (qs); sources of type 1-2 comprise the second group and show no evidence for the presence of such a spectrum. The last group is made of sources that belong to type 5. In the lower row of Figure 11 we show the same distributions for the variability equipartition Doppler factors, D.

From these plots it can be seen that at all bands there is a separation between the distribution of the first group when compared with the other two ones. This could be explained as follows; for sources of type 1-2 or 5 the dominance of flares relative to the quiescent spectrum is significant. Given the fact that the brightness temperature and the corresponding

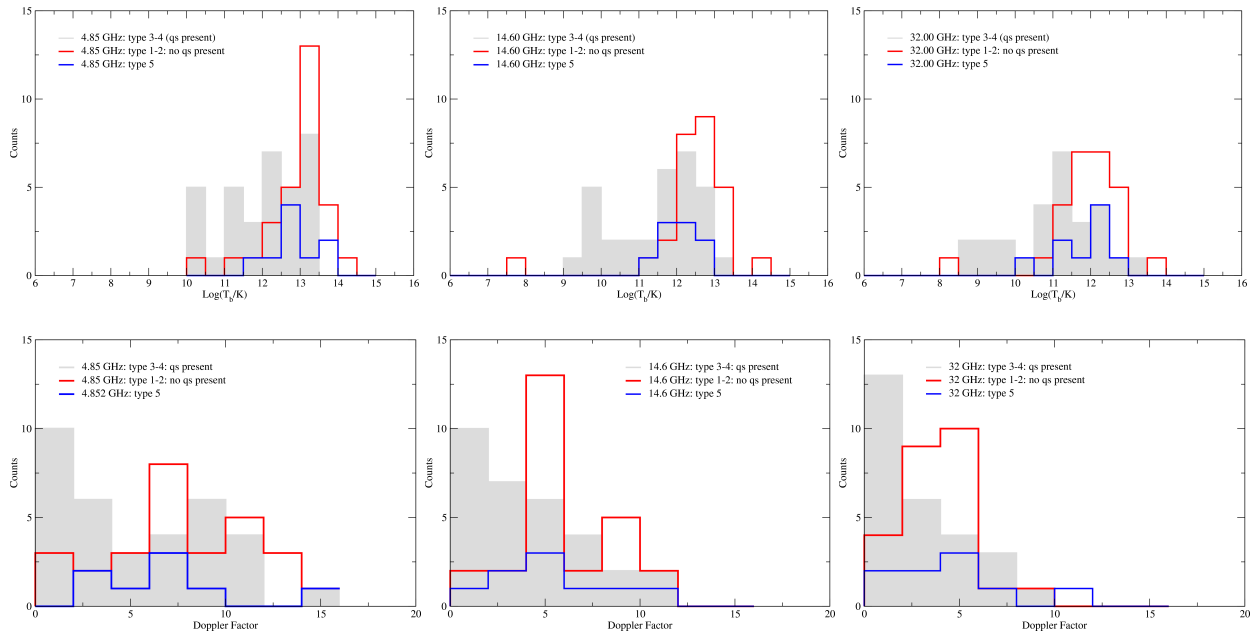


FIG. 11: Variability brightness temperatures and the inferred equipartition Doppler factor distributions. *Red* denotes sources of variability type 1-2 that show no clue of quiescent spectrum. *Grey* denotes sources where there is an evident quiescent spectrum and *blue* are sources of type 5. *Left*: 4.85 GHz, *middle*: 14.6 GHz, *right*: 32 GHz.

Doppler factor are inferred from the variability properties, it is naturally expected that sources where the quiescent spectrum is absent, show more pronounced variability characteristics. At the highest frequencies this separation must disappear due to the absence of quiescent spectrum.

IV. JET EMISSION FROM NLSY1S

Narrow Line Seyfert 1 galaxies are an AGN subclass that have been argued to show comparably low masses and high accretion rates [e.g. 16–19]. Only a mere 7% of them appears to be radio loud [20].

The early *Fermi* discovery of γ -ray emission from a small number of NLSy1s [21, 22]) came as surprise; until then the only γ -ray bright classes were thought to be blazars (i.e. FSRQs and BL Lac objects) and radio galaxies (for a review, see [23]). The discovery of γ -ray emission from NLSy1s not only introduced a new class of γ -emitting AGNs but also revolutionised the well spread belief that jets are associated (chiefly) with large elliptical galaxies. The multi-wavelength campaign between March and July 2009 following the discovery of γ -ray emission from PMN 0948+0022 showed that the source was exhibiting a spectral behaviour typical of a relativistic jet [24, 25].

Responding to the *Fermi* detection the *F-GAMMA* team initiated a dedicated program, to understand their cm to mm behaviour [26]. The three sources

TABLE I: The NLSy1 monitored by the *F-GAMMA* program.

Source	z	N^\dagger	f^\ddagger (months)	$\langle S_{4.85} \rangle$ (Jy)
1H 0323+342	0.061	18	1.0	0.40
PMN J0948+0022	0.585	42	0.9	0.23
PKS 1502+036	0.409	18	0.9	0.52

$^\dagger N$: number of observed epochs until February 2012

$^\ddagger f$: mean sampling

that are monitored are listed in Table I. In the following we discuss first results of this monitoring.

A. Radio Variability

In Figure 12 we show the variability light curves as well as the broad-band spectra observed within the context of the *F-GAMMA* program. For 1H 0323+342 and PMN J0948+0022 light curves between 2.6 and 142 GHz have been constructed while the steepening of the spectrum above 32 GHz in the case of PKS 1502+036, does not allow IRAM observations at short-mm bands.

1H 0323+342: As it can be seen in Figure 12, its radio spectrum displays a quiescent part reaching up to roughly 10 GHz beyond which a high frequency

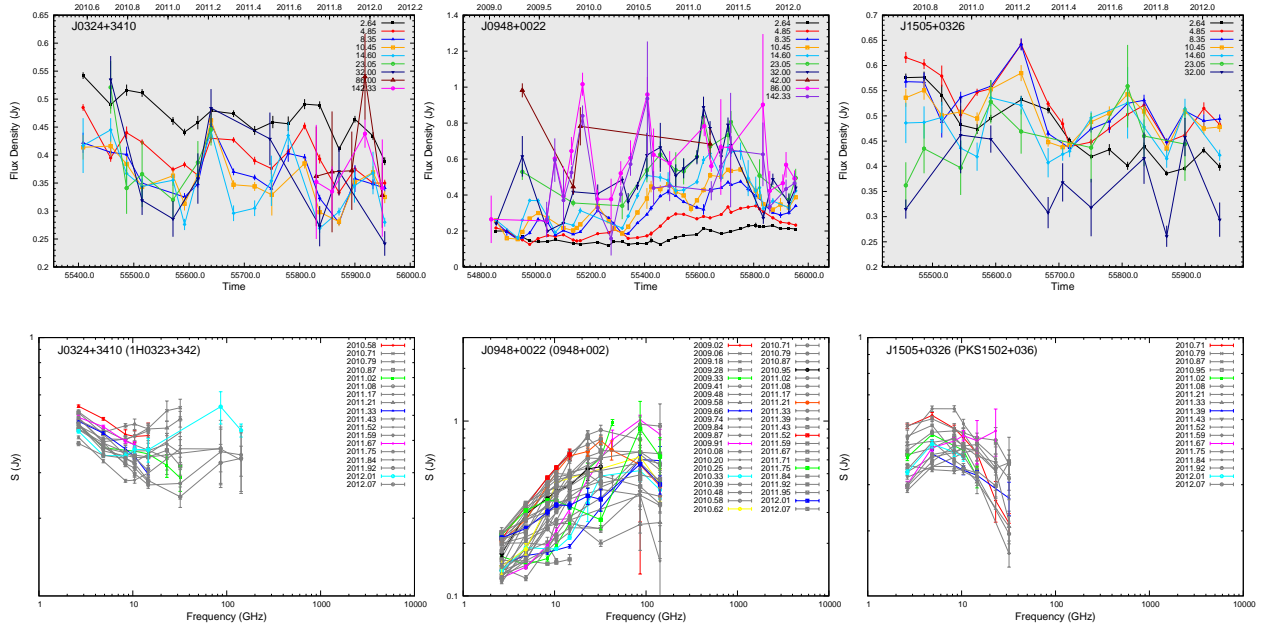


FIG. 12: Monthly sampled spectra and light curves for the three monitored NLSy1s. *Upper row*: the light curves at all *F-GAMMA* frequencies between 2.64 and 142 GHz. *Lower row*: the broad-band *F-GAMMA* spectra.

component (hereafter HFC) appears. Its mean spectral index is of the order of -0.23 (calculated between 2.6 and 10 GHz), not very different from a typical value of -0.5 ($S \propto \nu^\alpha$). The HFC shows intense spectral evolution which gradually shifts its peak progressively towards the steep spectrum component. The pace of the evolution is remarkably fast causing significant displacements within the month that typically separates two observations. The variability pattern according to the classification discussed in Sect. III A, is of type 4. Its light curves although only shortly sampled, shows a collection of events more prominent at higher frequencies and with cross-band lags indicative of the spectral evolution superimposed on a long term decreasing trend. The modulation index m ($m[\%] = 100 \times \frac{\sigma}{\langle S \rangle}$) at 4.85 GHz is, $m_{4.85} \approx 10\%$, while at 14.6 and 32 GHz it is, 17% and 27%, respectively. The *Structure Function* analysis applied on the source light curves revealed characteristic times scales of the order of 60 days which implies a variability brightness temperature of 10^{12} K at 4.85 GHz and 2×10^{11} K at 14.6 GHz. The corresponding equipartition Doppler factors are 2.4 and 1.5 respectively, placing the source in the lower part of the Doppler factor distribution shown in Figure 12. Interestingly, the Doppler factor calculated from fitting the Spectral Energy Distribution (SED) [21] is around 17.

PMN J0948+0022: It is evident from the light curves and the spectra shown in Figure 12 that the available dataset for PMN J0948+0022 is much

richer than that for the other two NLSy1s. The spectrum appears mostly inverted representative of variability type 1. The spectral index below 10 GHz ranges between marginally steep or flat (≈ -0.1) to highly inverted reaching values of $+1.0$. Its evolution is exceptionally dynamic with significant evolution happening even within one month. It appears that for this source a sampling of two weeks would be necessary. Its light curve shows at least 4 prominent events which emerge with time lags at different bands. At the lowest frequencies the events are barely seen. Yet, the modulation index shows a monotonic increase with frequency. At 2.6, 4.85, 14.6, 32 and 142 GHz the modulation index is 22, 29, 35, 37 and 38%, respectively. The standard variability analysis reveals brightness temperatures of 8×10^{12} K at 4.85 GHz, 2×10^{12} K at 14.6 GHz and 1.5×10^{11} K at 32 GHz which would imply rather typical Doppler factors of 6, 4 and 2 respectively, as it can be seen from the Doppler factor distribution plots in Figure 11. The SED modelling gives Doppler factors that vary between 10 and 20 with the latter being observed during the outburst of July 2010 [27].

PKS 1502+036: This source shows a variability behaviour similar to type 1b although more epochs are needed for a definite classification. Its spectrum is highly variable displaying periods of convex shape. Its low-band part ($\nu \leq 8$ GHz) varies between flat and highly inverted, while the higher frequencies ($10 \text{ GHz} \leq \nu$) can show spectral index as steep as -0.5 . The light curve shows at least 2

events better seen at higher frequencies. The high frequency cut-off of the spectrum prohibits IRAM monitoring. The typical time scales identified here are of the order of 60 - 80 days. At 4.85 GHz the brightness temperature is 2×10^{13} K and at 14.6 GHz it is 3×10^{12} K implying Doppler factors of 7 and 4, respectively while the SED fitting gives a value of 18.

B. Conclusions

From the above discussion it becomes obvious that the three monitored NLSy1s show a very typical blazar-like behaviour. That is, highly variable spectra caused by the presence of prominent evolving high frequency spectral components. The variability happens at interestingly fast pace with the mean number of events per unit time being clearly larger than that of the rest of the *F-GAMMA* targets. As an example, PMN J0948+0022 shows, on average, 1.4 flaring events per year as compared to less than ~ 1 event per year for other typical *F-GAMMA* blazars. The variability brightness temperature is relatively high with respect to the distribution of the whole sample in the cases of PMN J0948+0022 and PKS 1502+036. The opposite is the case for 1H0323+342. The derived Doppler factors are lower limits and are systematically lower than the values obtained from the SED

modelling. In any case, it seems premature to draw any final conclusions for the behaviour of this limited sample of NLSy1s. Longer time baselines will allow more accurate estimates of the brightness temperatures and all the variability parameters.

Acknowledgments

Based on observations with the 100m telescope of the MPIfR (Max-Planck-Institut für Radioastronomie) and the IRAM 30m Telescope. IRAM is supported by INSU/CNRS (France), MPG (Germany) and IGN (Spain). I. Nestoras and R. Schmidt are members of the International Max Planck Research School (IMPRS) for Astronomy and Astrophysics at the Universities of Bonn and Cologne. E. Angelakis wholeheartedly thanks Dr. A. Kraus for the constant support and the constructive discussions and Dr. T. Savolainen for all the usefull comments. Finally, E. Angelakis thanks the LOC and the SOC of the “*Fermi and Jansky: Our Evolving Understanding of AGN*” conference, for organizing such an interesting meeting and the anonymous referee for the thorough reading of the paper and the constructive comments.

-
- [1] A. P. Marscher and W. K. Gear, *ApJ* **298**, 114 (1985).
 - [2] M. Spada, et al., *MNRAS* **325**, 1559 (2001), arXiv:astro-ph/0103424.
 - [3] M. Villata and C. M. Raiteri, *A&A* **347**, 30 (1999).
 - [4] M. Boettcher, ArXiv e-prints (2010), 1006.5048.
 - [5] M. Boettcher and C. D. Dermer, in *Bulletin of the American Astronomical Society* (2010), vol. 42 of *Bulletin of the American Astronomical Society*, pp. 706–+.
 - [6] W. B. Atwood, et al., *ApJ* **697**, 1071 (2009), 0902.1089.
 - [7] L. Fuhrmann, et al., in *The First GLAST Symposium*, edited by S. Ritz, P. Michelson, and C. A. Meehan (2007), vol. 921 of *American Institute of Physics Conference Series*, pp. 249–251.
 - [8] E. Angelakis, et al., *Memorie della Societa Astronomica Italiana* **79**, 1042 (2008), 0809.3912.
 - [9] E. Angelakis, et al., ArXiv e-prints (2010), 1006.5610.
 - [10] E. Angelakis, et al., ArXiv e-prints (2011), 1111.6992.
 - [11] E. Angelakis, et al., ArXiv e-prints (2012), 1202.4242.
 - [12] Y. Y. Kovalev, et al., *PASA*, **19**, 83 (2002).
 - [13] J. H. Simonetti, et al., **296**, 46 (1985).
 - [14] A. C. S. Readhead, *ApJ* **426**, 51 (1994).
 - [15] A. Lähteenmäki, et al., *ApJ* **511**, 112 (1999).
 - [16] T.A. Boroson, in: “Narrow-Line Seyfert 1 Galaxies and Their Place in the Universe”, Milano (Italy), 4-6 April 2011, Proceedings of Science vol. NLS1, p. 003 (2011).
 - [17] D. Grupe, in: “Narrow-Line Seyfert 1 Galaxies and Their Place in the Universe”, Milano (Italy), 4-6 April 2011, Proceedings of Science vol. NLS1, p. 004 (2011).
 - [18] S. Mathur, in: “Narrow-Line Seyfert 1 Galaxies and Their Place in the Universe”, Milano (Italy), 4-6 April 2011, Proceedings of Science vol. NLS1, p. 035 (2011).
 - [19] B.M. Peterson, in: “Narrow-Line Seyfert 1 Galaxies and Their Place in the Universe”, Milano (Italy), 4-6 April 2011, Proceedings of Science vol. NLS1, p. 032 (2011).
 - [20] S. Komossa, et al., *AJ* **132**, 531 (2006), arXiv:astro-ph/0603680.
 - [21] A. A. Abdo, et al., *ApJL* **707**, L142 (2009), 0911.3485.
 - [22] A. A. Abdo, et al., *ApJ* **699**, 976 (2009), 0905.4558.
 - [23] L. Foschini, in: “Narrow-Line Seyfert 1 Galaxies and Their Place in the Universe”, Milano (Italy), 4-6 April 2011, Proceedings of Science vol. NLS1, p. 024 (2011).
 - [24] A. A. Abdo, et al., *ApJ* **707**, 727 (2009), 0910.4540.
 - [25] M. Giroletti, et al., *A&A* **528**, L11 (2011), 1102.3264.
 - [26] L. Fuhrmann et al., in: “Narrow-Line Seyfert 1 Galaxies and Their Place in the Universe”, Milano (Italy), 4-6 April 2011, Proceedings of Science vol. NLS1, p. 026 (2011).
 - [27] L. Foschini, et al., *MNRAS* **413**, 1671 (2011), 1010.4434.